



## Nanoparticle eluting-angioplasty balloons to treat cardiovascular diseases

Roshni Iyer<sup>a</sup>, Aneetta E. Kuriakose<sup>a</sup>, Serkan Yaman<sup>a</sup>, Lee-Chun Su<sup>a</sup>, Dingying Shan<sup>b</sup>, Jian Yang<sup>b</sup>, Jun Liao<sup>a</sup>, Liping Tang<sup>a</sup>, Subhash Banerjee<sup>c,d</sup>, Hao Xu<sup>a,c,\*</sup>, Kytai T. Nguyen<sup>a,\*</sup>

<sup>a</sup> Department of Bioengineering, University of Texas at Arlington, Arlington, TX, USA

<sup>b</sup> Department of Biomedical Engineering, Materials Research Institute, The Huck Institutes of the Life Sciences, Pennsylvania State University, University Park, PA, USA

<sup>c</sup> Department of Internal Medicine, University of Texas Southwestern Medical Center, Dallas, TX, USA

<sup>d</sup> Division of Cardiology, VA North Texas Medical Center, Dallas, TX, USA

### ARTICLE INFO

#### Keywords:

Drug eluting balloons  
Angioplasty balloon coating  
Nanoparticle coating  
Hydrogel  
Layer-by-layer

### ABSTRACT

Nanoparticles (NPs) can be used to locally deliver anti-restenosis drugs when they are infused directly to the injured arteries after intervention procedures such as angioplasty. However, the efficacy of transferring NPs via infusion to the arterial wall is limited, at least partially, due to poor NP retention on the inner artery wall. To improve NP retention, angioplasty balloons coated with drug-loaded NPs were fabricated via either layer-by-layer (LbL) electrostatic coating or acrylic-based hydrogel (AAH) coating techniques. Three types of NPs, namely poly (lactide-co-glycolide) (PLGA), biodegradable photo-luminescent PLGA and urethane doped polyester were studied. The transfer efficacy of NPs from various coatings to the arterial wall were further evaluated to find the optimal coating conditions. The *ex vivo* NP transfer studies showed significantly more NPs being transferred to the rat arterial wall after the angioplasty procedure by the AAH coating (95% transfer efficiency) compared to that of the LbL technique (60%) and dip coating (20%) under flow conditions (10 dyn/cm<sup>2</sup>). Our results suggest that the AAH coating of drug-loaded NPs on the angioplasty balloon could potentially provide superior retention of drug-loaded NPs onto the arterial wall for a better local delivery of drug-loaded NPs to effectively treat arterial diseases.

### 1. Introduction

Coronary artery disease (CAD) is a leading cause of death in developed countries, accounting for approximately 1 in 6 deaths in the United States and nearly 1 million cases of heart attack every year (Roger et al., 2012). Percutaneous transluminal coronary angioplasty (PTCA) is the prominent treatment modality for severe CAD blockage, and drug eluting stents (DES) are often used to support the arterial wall, treat flow-limiting coronary stenosis, and reduce the risk of restenosis. However, DES or bare metal stents suffer from several limitations such as the presence of permanent metal within the artery, incomplete stent apposition, and late in-stent thrombosis and restenosis (Agustina Rodriguez-Granillo et al., 2011).

Drug eluting balloons (DEB) are an alternative to DES particularly in conditions where stent use might not be optimal, such as at vessel bifurcations and small tortuous vessels (Waksman and Pakala, 2009). A few coronary artery DEB clinical trials have demonstrated their safety and efficacy in reducing restenosis (Byrne et al., 2013; Rittger et al., 2012). To date, the most common format for delivering drugs via DEB is by coating the drugs directly onto the balloon surface (Latib et al.,

2012; Fanggiday et al., 2008). Local delivery of drugs using angioplasty balloons serves as an alternative strategy to overcome limitations of drug delivery via a systemic route and infusion catheters. The drawbacks of systemic drug delivery include adverse drug toxicity and patient non-compliance. Infusion delivery involves the use of high pressure fluid jets to locally deliver drugs and/or drug-loaded NPs to the arterial wall; however, it might cause vascular trauma and leakage of drugs into non-desired areas like side branches of blood vessels (Song et al., 1998; Fram et al., 1994; Cyrus et al., 2008). Additionally, infusion delivery also suffers from non-homogenous NP transfer and poor NP retention within the arterial wall (Humphrey et al., 1997; Guzman et al., 1996). Drug eluting balloons overcome these limitations as they do not cause any additional vessel trauma beyond the angioplasty procedure (Waksman and Pakala, 2009; Kaule et al., 2015). In addition, coating drugs onto the balloon surface allows combined angioplasty treatment and local drug delivery. Upon balloon inflation, the inflation pressure causes the drugs coated on the balloon surface to be transferred to the arterial wall of interest. In an earlier clinical study, paclitaxel-coated balloons successfully inhibited restenosis and subsequent adverse cardiac events (Scheller et al., 2006). Other drug

\* Corresponding authors at: Department of Bioengineering, University of Texas at Arlington, 500 UTA Blvd, ERB 241, Arlington, TX 76019, USA.

E-mail addresses: [hao.xu@uta.edu](mailto:hao.xu@uta.edu) (H. Xu), [knguyen@uta.edu](mailto:knguyen@uta.edu) (K.T. Nguyen).

<https://doi.org/10.1016/j.ijpharm.2018.11.011>

Received 22 August 2018; Received in revised form 29 October 2018; Accepted 3 November 2018

Available online 05 November 2018

0378-5173/ © 2018 Elsevier B.V. All rights reserved.

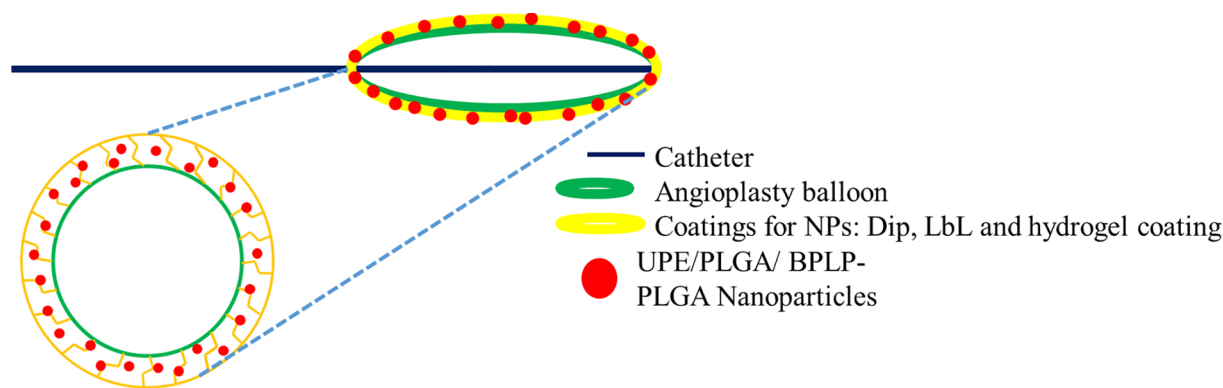


Fig. 1. Schematic of NPs coated on DEBs by hydrogel or layer-by-layer coating techniques.

coating and delivery techniques using DEBs such as liquid drug delivery with kissing balloons have also been explored (Rolland et al., 2003; Herdeg et al., 2008). Direct drug coating techniques have several limitations including poor drug loading onto the balloon, heavy drug loss during the balloon's passage through the blood vessel, and poor drug binding to the vessels due to the blood flow, leading to reduced drug bioavailability (Waksman and Pakala, 2009). Furthermore, the short half-life of these drugs limits their bioavailability resulting in multiple dosage requirements, which can be overcome by incorporating them into NPs and then delivering these NPs to the diseased site locally (Labhasetwar et al., 1997).

Increasing evidence supports the idea that a coating of drug loaded nanoparticles (NPs) onto an angioplasty balloon surface is a promising approach to significantly enhance and prolong drug delivery to the arterial wall. Over the last few years, NPs made from biodegradable polymers such as poly (lactic-co-glycolic acid) (PLGA) have been increasingly used as drug delivery vehicles for sustained releases of both hydrophobic and hydrophilic drugs (Menon et al., 2014; Kona et al., 2012). Recently, researchers have been exploring the prospects of locally delivering drug loaded NPs to the arterial wall. The advantage of using NPs is that they provide sustained drug release locally and enhance treatment efficacy compared to that of a free drug infused from the balloon catheter (Westedt et al., 2002). One such technique is by coating NPs onto stents using the “layer-by-layer” electrostatic self-assembly technique, which consists of alternate coatings of positively and negatively charged electrolytes (Nakano et al., 2009). Stents coated with NPs using electrodeposition were also able to deliver fluorescein-isothiocyanate (FITC) within the vessel wall up to four weeks (Nakano et al., 2009).

In addition to coating onto stents, NPs can be delivered to the blood vessel wall via an infusion catheter. Dexamethasone loaded biodegradable PLGA NPs were delivered locally to the arterial wall via infusion through commercial balloon catheters. This technique provided successful penetration of the NPs into the vessel wall and subsequently reduced neointimal growth (Guzman et al., 1996). Wilensky et al. (Wilensky et al., 1995) developed and evaluated the delivery of cerium-114 radiolabeled NPs using a porous balloon catheter, and found over 90% NP retention within seven days, indicating the potential application and advantage of local NP delivery. Our group has previously developed PLGA NPs encapsulating dexamethasone and surface conjugated with glycoprotein Ib- $\alpha$  (GPIb $\alpha$ ), which can selectively target P-selectin and vWF overexpressed on injured endothelial cells (ECs) and/or sub-endothelium layer of the arterial walls (Kona et al., 2012). These NPs successfully bound onto the injured arterial wall; thus, blocking the platelet binding sites on the endothelial cells and preventing inflammation. In addition, we have also developed citrate-based urethane-doped polyester (UPE) NPs functionalized with GPIb $\alpha$  and anti-CD34 antibodies to bind onto the injured endothelium and capture circulating endothelial progenitor cells for facilitating endothelium regeneration *in situ* (Su et al., 2014). These NPs compete

with platelets under flow conditions for binding sites by reducing platelet deposition and adhesion by about 50%. Additionally, these NPs, when delivered via infusion, could capture circulating human endothelial progenitor cells (HEPCs) and promote re-endothelialization of an injured blood vessel *in vivo*.

Our goal is to develop an angioplasty balloon device coated with drug loaded NPs to provide prolonged, sustained and maximal drug delivery to the arterial wall during the angioplasty procedure. This new device would perform interventional angioplasty treatment, while providing local delivery of drug-loaded NPs, thereby producing a high drug efficacy with a reduced drug dosage for therapeutic efficacy. We had previously designed and investigated NPs made of PLGA 50:50 (a well-studied, FDA approved biodegradable polymer) (Menon et al., 2014), UPE (Su et al., 2014), and biodegradable photoluminescent-PLGA (BPLP-PLGA) copolymer (Wadajkar et al., 2012; Hu et al., 2016). UPE is a biodegradable polymer with abundant carboxyl and hydroxyl functional groups available for ligand conjugation, whereas BPLP-PLGA allows *in-situ* visualization of the NPs due to its intrinsic fluorescent properties. In this study, we aim to examine NPs made of either PLGA 50:50, UPE or BPLP-PLGA 50:50 polymers and two different NP coating techniques, a conventional layer-by-layer coating (LbL) and a hydrogel coating (Fig. 1), to find the optimal NP coating combination to deliver drug loaded NPs to the injured arterial wall. Various aspects of NP coating on the balloon surface, including effects of NP concentration and incubation time on the NP coating efficiency and NP transfer effectiveness to the vessel wall, were studied using *in vitro* and *ex vivo* experiments for this optimizing process.

## 2. Materials and methods

### 2.1. Materials

Medical grade Sprinter Legend angioplasty balloons (3 mm  $\times$  1.5 mm) manufactured by Medtronic Inc. were used as received. PLGA 50:50, Acrylic acid (99%), ethylene glycol dimethacrylate, ammonium persulfate, and N, N, N', N'-Tetramethylethylenediamine, poly (vinyl alcohol) (PVA, 87–89% hydrolyzed), 1, 4-Dioxane, Coumarin-6, and Poly (allylamine) hydrochloride were all purchased from Sigma Aldrich Inc. MTS and LDH assay kits were bought from Promega Inc.

### 2.2. Nanoparticle fabrication and characterization

UPE was synthesized in our laboratory as described elsewhere (Dey et al., 2008). UPE NPs were prepared by a precipitation technique. In brief, 10% w/w of Bovine Serum Albumin (BSA) solution was added to 5 mL of UPE polymer solution (1% w/v in dioxane) to form the first emulsion. This emulsion was then added dropwise into a PVA solution (0.1% w/v in DI water) under constant stirring. After overnight stirring, the NPs were collected by centrifugation and lyophilization.

BPLP-PLGA 50:50 was synthesized as described previously (Hu et al., 2016). PLGA 50:50 and BPLP-PLGA 50:50 (1:100) NPs were

prepared by a standard double emulsion technique (Menon et al., 2014). Briefly, a 10% w/w BSA solution was added to a solution of 3% w/v of either PLGA 50:50 or BPLP-PLGA 50:50 in Dichloromethane (DCM) and sonicated using a microtip sonicator at 20 W for 1 min. This solution was then added dropwise to 5% w/v PVA solution (12 mL) and sonicated on ice using an ultrasonicator at 30 W for 10 min. Following overnight stirring, the NPs were washed with DI water and collected by centrifugation and lyophilization. UPE, PLGA 50:50 and BPLP-PLGA 50:50 NPs loaded with coumarin-6 (C-6) fluorescent dyes were also synthesized during the NP fabrication using the protocol as stated above following a slight modification, where 5% w/w C-6 was directly added to the polymer solution.

Particle size, size distribution, and surface charges were measured using the Dynamic Light Scattering (DLS) technique via the ZetaPALS zeta potential analyzer (Brookhaven Instruments Inc.). BSA (model protein) loading efficiency for each NP was determined by an indirect method. Briefly, BSA in the supernatant formation process was quantified by Bicinchoninic protein assays (BCA, Pierce) and a UV-Vis spectrophotometer (Infinite M200 Tecan Group Ltd) at 562 nm. The amount of BSA loaded into the NPs was determined by the following formula;

$$\% \text{ BSA loading} = \frac{\text{BSA amount used} - \text{BSA in supernatant}}{\text{BSA amount used}} * 100$$

The amount of C-6 loaded into the NPs was determined by a direct loading efficiency method. Briefly, 1 mg of NPs were dissolved in 1 mL of DCM, followed by the addition of 4 mL of 100% ethanol to separate coumarin-6 from the NPs. This solution was then centrifuged, and the amount of coumarin-6 in the ethanol phase was quantified by measuring the fluorescence of C-6 at Excitation: 458 nm and Emission: 540 nm using a UV-Vis spectrophotometer and used to provide the amount of C-6 loaded in 1 mg NPs. The amount of C-6 loaded into the total weight of NPs obtained after lyophilization was determined, and the loading efficacy was calculated by the following formula;

$$\% \text{ C-6 loading} = \frac{\text{Total C-6 amount in NPs}}{\text{C-6 amount used}} * 100$$

To study the BSA release kinetics from the NPs, the lyophilized NPs were re-suspended in DI water in a 1 mg/ml concentration. The NP suspension was added to a dialysis bag (100 kDa molecular weight cut-off, Spectrum Laboratories) and incubated in DI water for about 25 days at 37 °C. At pre-determined time points, dialysates were collected and frozen for later analysis, and the samples were replenished with fresh DI water. The amount of BSA released was quantified by protein assays and UV-Vis absorbance at 562 nm (Infinite M200 plate reader, Tecan). A standard curve of known BSA concentrations and the respective loading efficiencies of each NP (amount of drug released was normalized against the respective drug loaded into the NPs) were used to determine the cumulative BSA release.

We used a centrifugation technique to study the release kinetics of C-6. Briefly, C-6 loaded NPs were resuspended in DI water at a concentration of 1 mg/mL and incubated at 37 °C for 25 days. At pre-determined time-points, the NP suspension was centrifuged to collect the supernatant (containing the released drug). The NP pellet was re-suspended in DI water and returned to 37 °C until the next time-point. To quantify the drug in the supernatant for each time-point, 1 mL of 100% DMSO was supplemented to dissolve the C-6. The amounts of coumarin-6 released from the NPs were quantified by measuring the fluorescence of coumarin-6 at Excitation: 458 nm and Emission: 540 nm using a UV-Vis spectrophotometer for each sample. Drug release (%) of BSA and coumarin-6 were calculated by the formula below, followed by quantifying the cumulative drug release, which is the amount of drug released from the beginning of the study to the current time-point.

Formula for determining the amount of drug released from the NPs are as below:

$$\begin{aligned} & \text{A) Concentration of drug released from NPs (mg/mL)} \\ & \quad (\text{absorbance or fluorescence of drug}) \\ & = \frac{\pm \text{intercept from the standard equation}}{\text{slope from the standard equation}} \end{aligned}$$

The standard equation is obtained from the standard curve with the y axis as absorbance or fluorescence intensities of standard samples and x axis as standard concentrations

$$\text{B) Amount of drug released (mg) = Concentration of drug released from NPs (mg/mL) * dilution factor (mL)}$$

C) % of drug released from NPs:

$$\% \text{ of drug released from NPs} = \frac{\text{Amount of drug released from the NPs}}{\text{Amount of drug loaded into those NPs}} * 100$$

$$\text{D) Cumulative drug release} = (\%) P(t_z - 1) + P(t_z)$$

where,  $P(t_z)$  = Percentage of drug released from NPs before time 'z' to time 'z'

$P(t_z - 1)$  = Percentage of drug released from the NPs before time 'z'

The biodegradable nature of the NPs was examined by determining changes in the nanoparticle weight over time at 37 °C. To study the degradation profile, 2 mg of each NP type (non-drug loaded) was dissolved in 1 mL deionized water and incubated at 37 °C. At pre-determined time points, the NP suspension was centrifuged, followed by lyophilization of the pellet to collect the remaining product for weighing. The degradation profile was plotted as a percentage of weight of remaining NPs vs. time (days).

### 2.3. Coating of NPs on the angioplasty balloon surface

Two particle-coating techniques, layer-by-layer (LbL) coating and hydrogel coating, were used to coat the synthesized NPs on the balloon surface. In LbL coating, the inflated balloon was first immersed in a poly (allylamine hydrochloride) solution (PAH, 0.187% (w/v) in 0.5 M NaCl) for 30 min at room temperature to create a positively charged layer on the balloon surface. The balloon was then incubated in a NP suspension (mg/mL based on study) for 24 h to create a negatively charged layer on the balloon surface. The balloon was then air-dried and deflated for storage. UPE NP coatings on the balloon surface were also visualized by scanning electron microscopy imaging (SEM, Hitachi S-3000N variable pressure, Hitachi).

Hydrogel coated angioplasty balloons were developed by coating poly (acrylic acid) hydrogel onto the balloon surface. Poly (acrylic acid) hydrogel was synthesized by crosslinking acrylic acid using cross-linker ethylene glycol dimethacrylate (EGDMA) by a process described earlier (Jabbari et al., 2007). Briefly, 7.4 g of acrylic acid was dissolved in 7 g of water, to which 0.05 g EGDMA, 0.016 g of ammonium persulfate (APS), and 0.081 g Tetramethylethylenediamine (TEMED) were added, in that order, to initiate and accelerate the crosslinking process. The angioplasty balloons were then inflated at a pressure of 10 atmospheres; then the pre-hydrogel solution was added onto angioplasty balloons and complete gelation was allowed at 50 °C in an anaerobic condition by continuous nitrogen purging for about 1 h. After gelation, the balloons were air-dried before the next step. NPs were coated onto inflated hydrogel-coated balloons by immersing the balloon in a nanoparticle suspension for about 24 h, and then the balloons were air-dried and deflated for later use. UPE NP coatings on the balloon surface were visualized by SEM imaging. Control NP coated balloons were obtained by simply dip coating an inflated balloon in the NP suspension for 24 h without any excipients followed by air drying and deflation.

#### 2.4. Optimization of nanoparticle coating on the balloon surface

To optimize the system, several conditions including particle concentrations (0–1 mg/mL) and incubation times (0–48 h) during the process of NP coating were evaluated. The time and NP concentration at which the NP loading onto the balloons reached a plateau, i.e. the point after which no change in NP loading was observed, was the point of saturation for NPs loaded on the balloon surface. To perform the studies, particles were loaded with coumarin-6 fluorescent dyes to permit easy detection and fluorescence-enabled visualization of the nanoparticles coated onto the balloon and/or transferred to an artery (Finke et al., 2014).

The optimum duration for which the balloon was incubated in the nanoparticle suspensions was also investigated. Angioplasty balloons (N = 3) were incubated in 200 µg/mL particle suspensions at room temperature for various time points up to 48 h for each coating method. At each time point, balloons were removed from particle suspensions and the number of NPs loaded onto the balloons was measured on the basis of fluorescence exhibited by Coumarin-6 (excitation/emission: 458/540 nm). NP coating efficiency on the balloon was determined using the below formula. NP coating efficiency plotted against time was used to analyze the incubation time by which nanoparticle loading had reached its saturation.

To determine the effect of NP concentrations on the coating efficacy onto the balloon surface, increasing concentrations of NPs were first coated onto the balloon surface by either LbL or hydrogel coating technique. After 24 h of incubation in the NP suspension, the balloon was extracted, and the number of NPs coated on the balloon surface was determined as described above. The efficacy of NP coating on the balloon surface plotted against concentration was used to analyze the optimal concentration by which nanoparticle coating had reached its saturation. The efficiency of NP coating on the balloon was determined by the following formula;

$$\text{NP coating efficiency} = \frac{\text{Amount of NPs used} - \text{amount of NPs in supernatant}}{\text{Amount of NPs used}} * 100$$

#### 2.5. Cyto- and hemo-compatibility studies of nanoparticles and coatings

Cyto-compatibility of the NPs and coatings to human endothelial progenitor cells (HEPCs) were examined by cell viability MTS assays. EPCs were isolated from human blood using Histopaque®-1077 (Sigma) per the manufacturer's protocol. The mononuclear fraction was isolated by density gradient centrifugation, followed by cell culture in endothelial basal media-2 supplemented with EGM-2 SingleQuots (Lonza). To test the cyto-compatibility of the nanoparticles, HEPCs were seeded on a 96 well plate at an initial seeding density of 8,000 cells/well. After 24 h of incubation, the cells were exposed to either increasing concentrations of NPs, NPs coated via LbL coating or hydrogel coating with or without NPs (100 and 1000 µg/mL NP concentrations). 24 h post exposure to the nanoparticles or coatings, cell viability was assessed by MTS assays per the manufacturer's instructions and normalized to untreated cell samples (control).

Each coating strategy and the NPs were compared for hemo-compatibility by whole blood clotting and hemolysis assays. First, substrates of UPE NPs, LbL coated UPE NPs, hydrogel only and hydrogel loaded UPE NPs were prepared in 1.5 mL centrifuge tubes. 0.9% saline and water were considered as the negative and positive controls, respectively. For this study, 30 mL of fresh human blood was collected from a donor and placed into acid citrate dextrose anticoagulant (ACD) tubes following collection and handling methods approved by the Institutional Review Board at the University of Texas at Arlington. A total sample size of eight was used for the following studies.

To observe the blood clotting trend, 0.85 mL CaCl<sub>2</sub> (0.1 M) was added to 8.5 mL ACD blood to initiate blood clotting. Immediately, 50 µL of activated blood was added to the samples. At different time

points (10, 20, 30 and 60 min), 1.5 mL DI water was added, and the substrates were incubated for five minutes at room temperature. The lysates were then collected for each time point, and the absorbance for each lysate sample was measured in a transparent UV well plate at 540 nm using a UV-Vis spectrophotometer and plotted against time.

To measure hemolysis caused by the NPs and the coatings, hemolysis assays, as previously described, were performed (Dey et al., 2010). 200 µL of ACD blood was pipetted into two separate tubes: a positive control (a tube with 10 mL DI water) and a negative control (a tube with 10 mL 0.9% saline). To test the hemolysis of each sample, 200 µL of the saline diluted blood was added to 50 µL of each sample. The samples were then incubated at 37 °C for 2 h. The tubes were then centrifuged at 1000g for 10 min, and 200 µL of the supernatant was then transferred to a 96 well plate and the absorbance was read using a UV-Vis spectrophotometer at 545 nm. Hemolysis for the samples was quantified as below:

$$\% \text{ Hemolysis} = \frac{\text{Absorbance of sample} - \text{absorbance of negative control}}{\text{Absorbance of positive control}} * 100$$

#### 2.6. Ex vivo retention of nanoparticles on arterial wall under dynamic flow conditions

In this study, we quantified the amount of coumarin-6 loaded UPE nanoparticles retained on the arterial wall after balloon angioplasty under dynamic flow conditions using an *in vitro* closed-loop flow model adapted from Nguyen et al (Nguyen et al., 2003). Nanoparticle coated balloons via hydrogel, LbL and dip coatings were manufactured as described earlier. Uncoated balloons (no NPs) were used as controls. The number of NPs coated on the balloon was determined as described in the earlier section. To quantify the NP transfer efficiency, first the coated or control balloons were inserted into a rat arterial segment of 2 cm in length. NPs were transferred by inflating and deflating the balloon within the artery three times at a pressure of 10 atmospheres. The arteries mounted between silicon rubber tubings (1.6 mm ID, wall thickness 0.8 mm, Nalgene) were perfused with 6% dextran solution as a blood substitute in a closed-loop system (Waxman et al., 1985), at a physiological relevant shear stress (10 dyne/cm<sup>2</sup>) generated by a peristaltic pump (Cole-Parmer). The wall shear stress for the arterial segment was calculated from the following equation:

$$\tau = \frac{32\mu Q}{\pi d^3}$$

where Q is the volumetric flow rate,  $\mu$  is the fluid viscosity, d is diameter of the arterial segment (Papaioannou and Stefanadis, 2005). Following five minutes of perfusion under flow conditions, the arteries were immediately collected and imaged using a fluorescence imager to visualize the nanoparticles retained in the blood vessel after the perfusion. Post-imaging, the arteries were homogenized in a tissue homogenization buffer (1 mM Ethylenediaminetetraacetic acid (Sigma), 10 mM Tris-hydrochloride (Sigma) at pH 7.2) and centrifuged to collect the accumulated nanoparticles. The efficiency of NP transfer to the artery was determined directly using the formula:

$$\text{NP transfer efficiency} = \frac{\text{Amount of NPs transferred to the artery}}{\text{Amount of NPs coated on the balloon}} * 100$$

#### 2.7. Statistical analysis

Results were analyzed statistically using 2-way ANOVA and Fisher's post-hoc analysis (Statview 5.0 software) with p < 0.05 considered as a significant value. All results are displayed as mean  $\pm$  SD, and triplicate samples were used for each experiment if not specified.

### 3. Results

#### 3.1. Characterization of nanoparticles:

Size (nm) and zeta potential (mV) (surface charge) of NPs were quantified using the Dynamic Light Scattering (DLS) system. The average diameters of UPE, PLGA and BPLP-PLGA NPs were about 300, 182, and 220 nm, respectively, while the average zeta potentials were  $-28$ ,  $-27$ , and  $-40$  mV, respectively (Fig. 2). Using bovine serum albumin (BSA) as a model protein, loading efficiencies of UPE, PLGA

and BPLP-PLGA NPs were found to be 67%, 52% and 65%, respectively. The BSA release profile illustrates an initial burst release followed by a sustained release of BSA over 25 days for most of the NP types (Fig. 3A(i)). In the case of BPLP-PLGA NPs, almost 100% of BSA was released within 7 days. PLGA and UPE, on the other hand, showed a slower drug release, with about 80% of BSA being released within 25 days because of a slower degradation rate of the polymers (Fig. 3B). Moreover, the release kinetics of BSA from UPE NPs were slower than those of BPLP-PLGA and PLGA. Thus, UPE NPs not only exhibited a superior loading efficiency, but also consisted of a slower and more

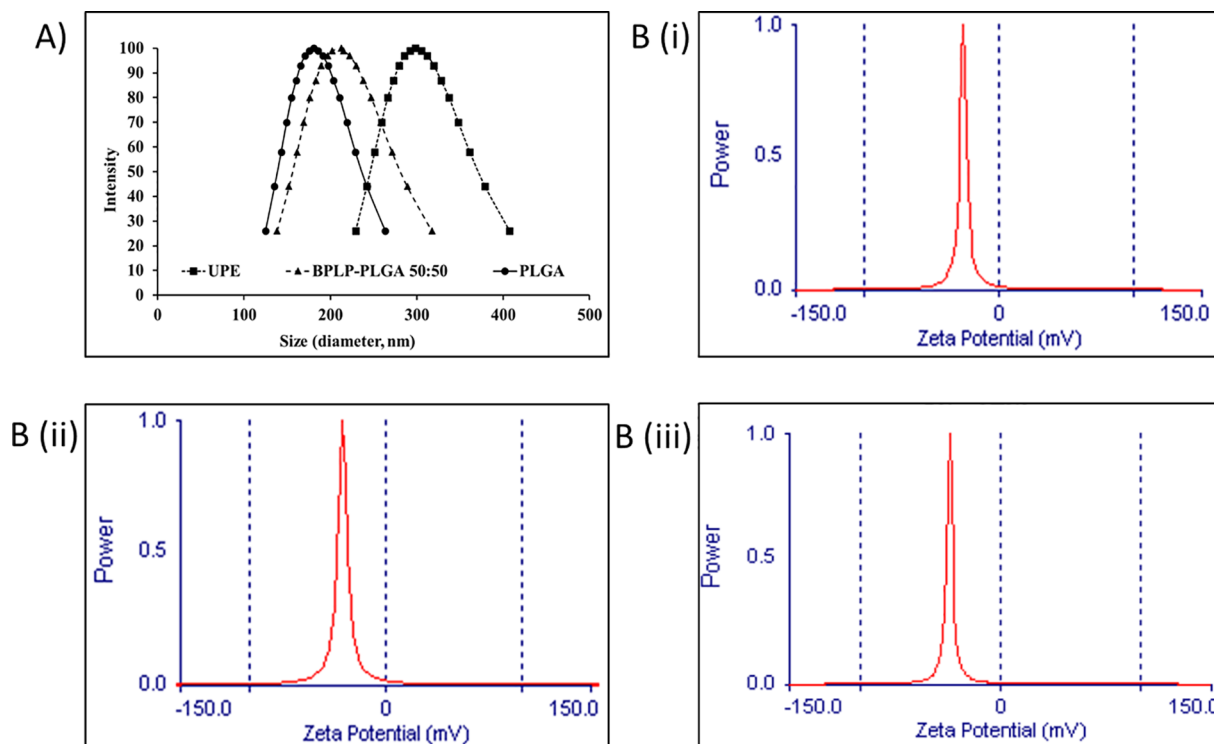


Fig. 2. Dynamic light scattering analysis of nanoparticles. (A) Hydrodynamic size distribution and (B) zeta potentials of (i) UPE NPs, (ii) PLGA NPs and (iii) BPLP-PLGA 50:50 NPs.

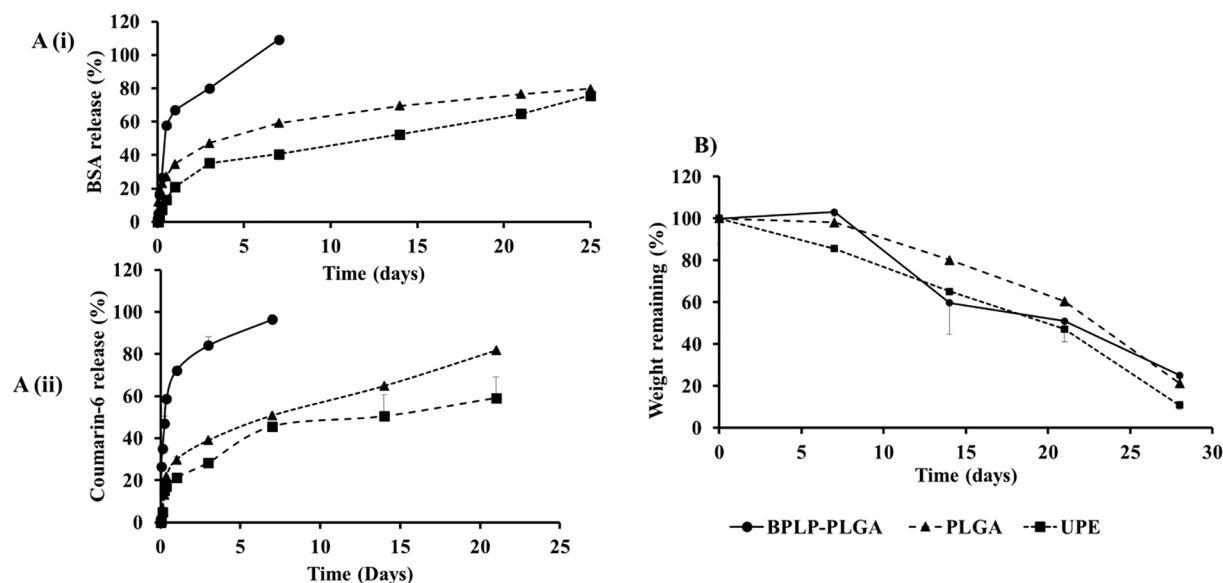


Fig. 3. Characteristics of nanoparticles. (A) Drug release profiles of (i) BSA and (ii) coumarin-6 from PLGA, UPE and BPLP-PLGA NPs show UPE nanoparticles displaying slower and more sustained drug release. (B) Degradation profiles of these nanoparticles show weight loss of the NPs with time indicating biodegradability.

sustained drug release. Similar release kinetics of coumarin-6 were observed for UPE and PLGA NPs, where an initial burst release of the drug (~30%) was followed by sustained release over 21 days (Fig. 3A(ii)). BPLP-PLGA NPs, on the other hand, exhibited a faster drug release similar to that of BSA, with nearly 100% of drug being released within 7 days. In addition, these NPs were degraded by 80% (weight loss) within 28 days (Fig. 3B). The complete drug release from the BPLP-PLGA NPs was observed within 7 days, whereas the BPLP-PLGA NP degradation up to 28 days could potentially be due to the leftover degradation products of the NPs that were detectable for longer durations. It is also important to note that, although almost 80% of the UPE and PLGA NPs were degraded by 28 days, the drug release profile of BSA from the NPs showed a slower drug release. Additionally, we also observed an incomplete BSA release from PLGA and UPE NPs despite nearly 80% weight loss by 28 days. We speculate that this observation could be a result of a longer time required for the drugs to diffuse from the NPs and the time needed for the polymer shell to erode before the drug is released from the core (Mu and Feng, 2003). Furthermore, the presence of residual PVA may add to the weight of the NPs, hence increasing the weight post degradation (Panyam et al., 2003).

### 3.2. Characterization of coatings

Nanoparticle coatings via LbL, hydrogel or dip coating (as control coating) on the balloon surface were first characterized by imaging techniques. Fig. 4A and B represent microscopy images of the angioplasty balloon with a UPE NP coating. Fig. 4B displays uniform coating of fluorescently labeled NPs on the balloon surface. Fig. 4C shows the balloon surface without coating (control) by scanning electron microscopy (SEM). Fig. 4D and E display successful loading of UPE NPs onto the balloon surface by SEM for dip and LbL coatings, respectively. Fig. 4F shows UPE NPs loaded onto a hydrogel coated balloon. While the LbL coatings show a more uniform coating of NPs on the balloon, the hydrogel coating resulted in a non-uniform loading of NPs onto the balloon surface. It is also important to note that although the SEM images demonstrate fewer NPs on the surface of the hydrogel coating, the swelling nature of the hydrogel may result in a higher NP loading into the hydrogel networks.

Optimization of the coating process was performed based on the NP concentration and the saturation time for NP loading onto the balloon surface. The results for the coating efficiency study indicate a significant difference in the saturation times and NP concentrations for the loading of NPs via hydrogel and LbL coatings. Fig. 5A and B depict the effects of incubation time for NPs (200 µg/mL) in the coating procedure for LbL and hydrogel coatings, respectively, wherein both coatings consistently loaded more NPs with an increase in time of incubation, reaching a plateau at 24 h (NP loading efficiency of about 75% and 63% of the initial 200 µg/mL of UPE NPs used, for the hydrogel and LbL methods, respectively after 24 h of incubation). Fig. 5C and D demonstrate the effects of NP concentrations on NP coating efficiency onto the balloon surface via LbL and hydrogel coatings, respectively upon a 24-hour incubation period. Hydrogel coatings consistently loaded a greater number of NPs onto the balloon compared to the LbL coating in a dose-

dependent fashion, reaching saturation at a NP concentration of 500 µg/mL. Additionally, UPE NPs showed superior NP loading efficiency by both coating strategies, especially the hydrogel coating compared to that of the LbL coating (about 90% and 76%, respectively at a NP concentration of 500 µg/mL). Based on these results, we have determined that the ideal parameters of the NP for coating onto the balloon surface are: a NP concentration of 500 µg/mL and 24 h of incubation time to formulate NP-eluting angioplasty balloons. Since UPE NPs displayed superior drug loading efficiency, more sustained drug release and a higher coating efficiency on the balloon surface, UPE NPs were used for further studies.

### 3.3. Cyto- and hemo-compatibility of nanoparticles and coatings

MTS assays were performed to evaluate the cytocompatibility of UPE NPs and the coatings with human endothelial progenitor cells (HEPCs). More than 80% of HEPCs were viable after 24 h of incubation with increasing concentrations of NPs (Fig. 6A) and coating substrates with or without UPE NPs (Fig. 6B), suggesting minimal toxicity of these NPs and coatings.

Fig. 7 shows the blood clotting profile and hemolysis (%) for the UPE NPs and coating strategies. The blood clotting profiles for low and high concentrations of UPE NPs and the hydrogel substrate (Fig. 7A) were observed to follow a trend similar to that of saline (control). As expected, blood clotting increased with time, with all of the samples clotting within 20 min. Additionally, UPE NPs demonstrated about 1% hemolysis even at high NP concentrations (0.1% and 1% for 0.1 and 1 mg/mL NP concentration, respectively) as shown in Fig. 7B. Similar results were observed in the hydrogel coating, where hydrogel by itself and hydrogels loaded with 0.1 mg/mL UPE NPs observed < 1% hemolysis (0.3% and 0.4%, respectively). Hydrogels loaded with 1 mg/mL UPE NPs displayed a slightly higher hemolysis than that of NPs (about 1.4%). The addition of UPE NPs to the hydrogel did not increase hemolysis significantly compared to that of hydrogel coatings alone. Importantly, the NPs and coatings observed hemolysis much below the acceptable hemolysis limit (Amin and Dannenfels, 2006). Thus, the nanoparticles and coating strategies used were confirmed to be cyto-compatible and hemo-compatible.

### 3.4. Ex vivo nanoparticle transfer efficiency

NPs transferred to the arterial wall via different coatings under flow were studied using *ex vivo* rat arteries and a fluorescence imager. This study focused on the efficacy of coating methods to transfer NPs encapsulated with fluorescent dyes (e.g. coumarin-6) to the arterial wall under flow conditions. Fig. 8A shows a schematic of the flow loop system that was used in the study. Fig. 8B depicts a fluorescence image of an artery, demonstrating that NPs were successfully transferred to the vessel wall. The higher the fluorescent intensity observed in the image, the more NPs were transferred to the vessel lumen. We found that hydrogel coatings could uniformly deliver NPs throughout the arterial segment (signal intensity of ~ 30,000 a.u.), while LbL and dip coating delivered fewer number of NPs, which was indicated by the diminishing

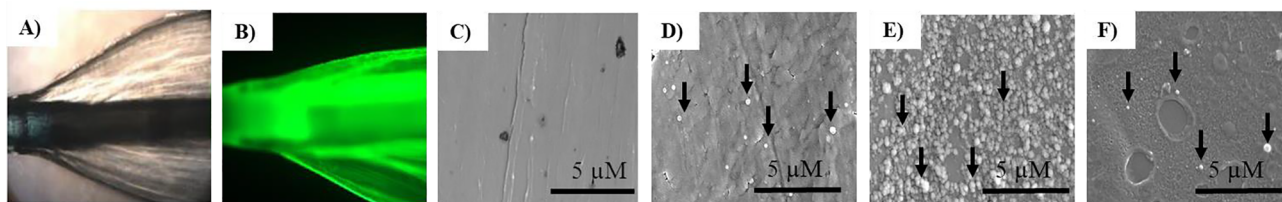


**Fig. 4.** Characterization of coatings. (A) and (B) microscopy images of balloon catheters coated with Coumarin-6 dye (green) loaded NPs, (C) SEM image of uncoated angioplasty balloons, (D) SEM image of angioplasty balloon coated with NPs via dip coating, (E) SEM image of angioplasty balloons coated with NPs via the LbL coating method, and (F) SEM image of angioplasty balloons coated with NPs via the hydrogel coating technique. UPE NPs were used in these images. (For interpretation of the references to colour in this figure legend, the reader is referred to the web version of this article.)

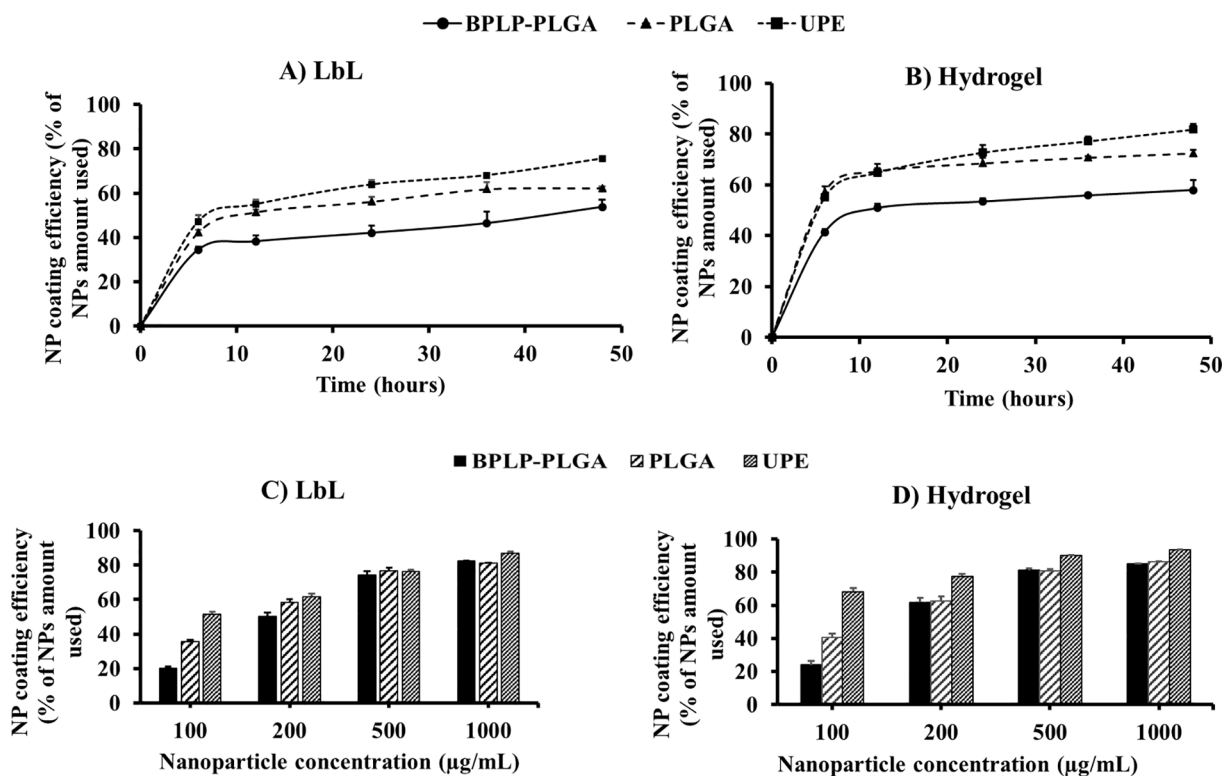


Fig. 5. Optimization of NP coating on angioplasty balloons. LbL coatings (A) and hydrogel coatings (B) displayed incubation time-dependent NP coating efficiency, where the coating reached a saturation within 24 h. LbL coatings (C) and hydrogel coatings (D) observed a concentration-dependent increase in NP coating efficiency, with UPE NPs showing higher coating efficiency compared to those of BPLP-PLGA and PLGA NPs. Additionally, the coating reached saturation at a NP concentration of 500 µg/mL for the hydrogel coatings. n = 3 replicates were used for these studies.

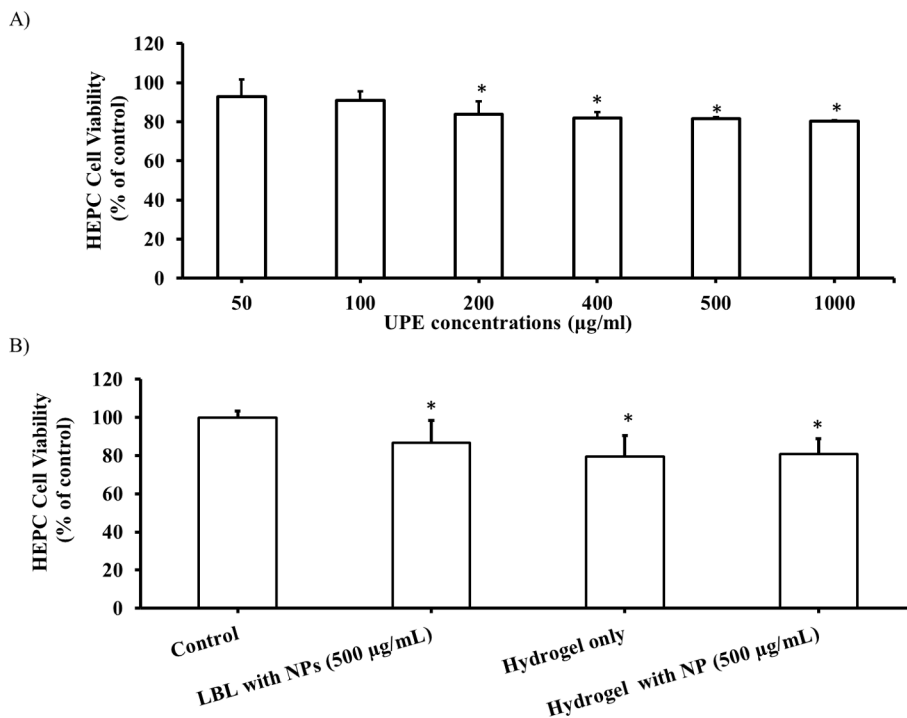


Fig. 6. Cytocompatibility of UPE NPs and coating substrates to HEPCs. (A) Increasing concentrations of UPE NPs and (B) NP coating substrates both show more than 80% HEPC viability after 24 h of exposure to the NPs and the coating substrates. \*p < 0.05 vs. control, n = 4 replicates were used for these studies.

fluorescence intensity in the arteries (signal intensity of ~20,000 a.u. for LbL coating and ~8,600 a.u. for dip coating). Fig. 8C highlights a significant difference in the nanoparticle transfer and subsequent retention efficiency in the arterial lumen, when comparing hydrogel and LbL

coatings to the dip coating. The NP transfer efficiencies were 95% for hydrogel coatings, 60% for LbL coatings, and 20% for dip coatings, indicating that hydrogel coated balloons could carry and transfer NPs to the arterial lumen more efficiently via balloon angioplasty.

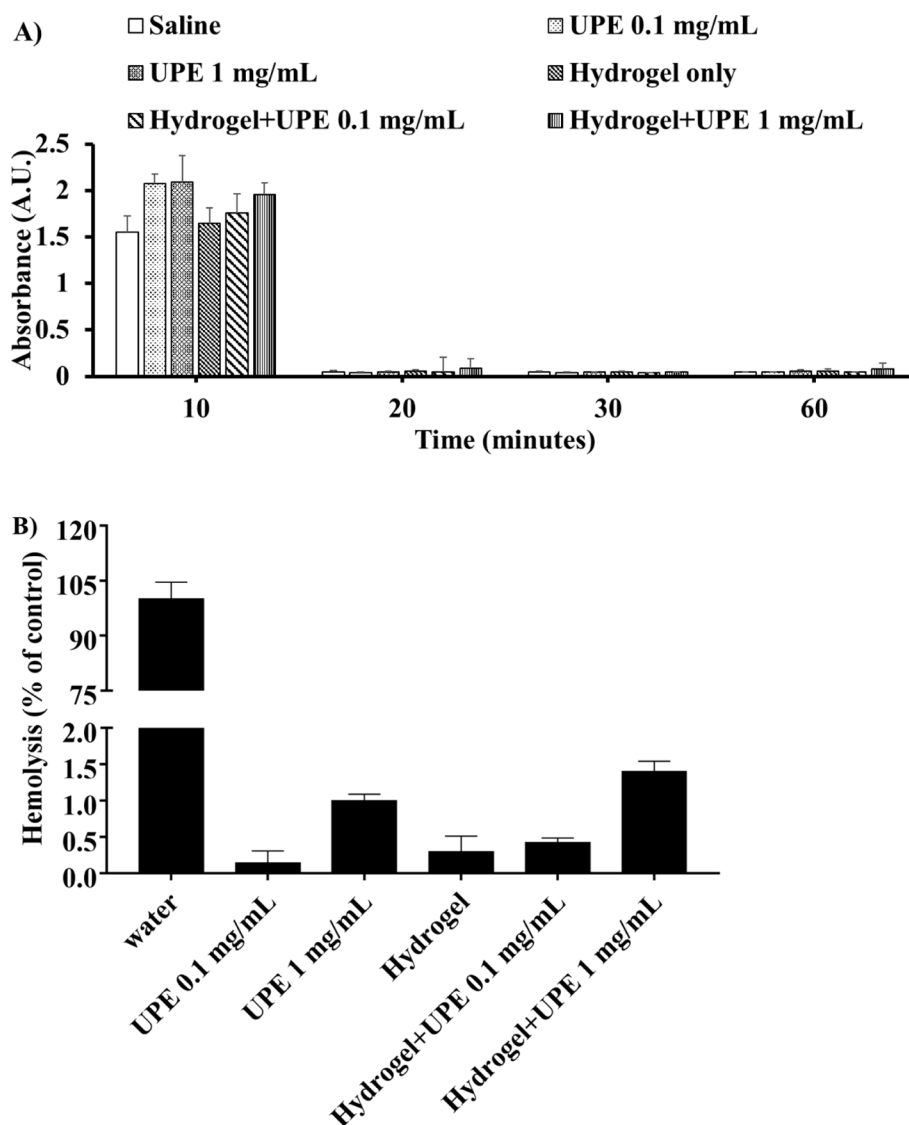


Fig. 7. Hemocompatibility of UPE NPs and coating substrates. (A) Blood clotting profiles of NPs and substrates were similar to that of saline control. (B) Hemolysis for the NPs and coating substrates was also observed to be < 2%. n = 8 replicates were used for these studies.

#### 4. Discussion

NPs for intravascular drug delivery have been vigorously investigated by many researchers due to certain advantages compared with systemic drug delivery. Major benefits of nanocarriers include; sustained release of therapeutic reagents, prolonged drug effects, protection against degradation of the encapsulated agents, and increased drug bioavailability (Panyam and Labhasetwar, 2003). Similar to previous studies of biodegradable polymeric NPs like PLGA (Menon et al., 2014; Kona et al., 2012; Vasir and Labhasetwar, 2006; Vasir and Labhasetwar, 2007), our results of drug release from PLGA NPs and UPE NPs also provide sustained releases of the encapsulated drugs over a month. Another advantage of NPs is that they can load different drug types, including unstable, lipophilic, and/or hydrophilic therapeutic reagents (Lin et al., 2010; Xu et al., 2013). In addition, modification of NPs with either peptides or antibodies has been found to increase cellular uptake in vascular cells and to enhance the particle retention on the arterial wall, leading to an increase in local drug bioavailability at the atherosclerotic vessels and an improvement in the drug delivery and treatment efficiency (Su et al., 2014; Vasir and Labhasetwar, 2006; Davda and Labhasetwar, 2002; Labhasetwar et al., 1998). These features are particularly prominent in the case of UPE NPs that display

many carboxyl and hydroxyl units, which provide a potential for conjugation of specific peptides and antibodies for binding onto the injured arterial wall after the NP transfer process. Additionally, our group has also observed UPE NPs to be highly cyto- and hemo-compatible; thus, rendering them advantageous for tissue engineering and drug delivery applications (Su et al., 2014).

Drug delivery to the injured arterial wall via NPs can potentially overcome the limitations of DES and DEB, such as limited drug loading and delivery from DES and rapid wash-off of therapeutic reagents from the DEB. Recently, Lemos et al. (Lemos et al., 2013) found that sirilimus-loaded nano-carriers delivered to the arterial regions via either a coronary stent-plus-balloon system or a stand-alone balloon transferred the drug to all layers of the arteries effectively. In this study, although drug concentrations in the arterial tissues decreased with time, they were still detectable up to 2 weeks after delivery, leading to the reduction of neointimal proliferation efficiently. The past decade has witnessed extensive use of commercially available hydrogel-coated balloons to locally deliver drugs like paclitaxel (Kaule et al., 2015), heparin (Azrin et al., 1994), and argatroban (Imanishi et al., 1997), among others. In our study, we observed that the hydrogel coatings showed significantly enhanced NP loading and more efficient NP transfer to the arterial wall compared to those of LbL and dip coatings.

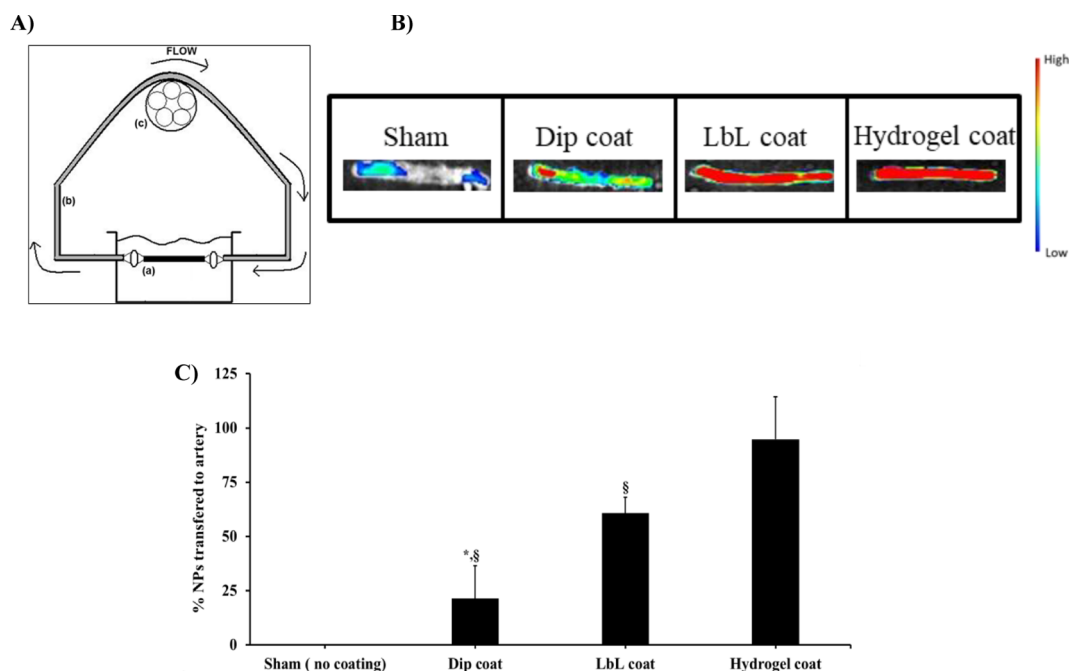


**Fig. 8.** *Ex vivo* UPE NPs transfer efficiency under flow conditions. (A) *In-vitro* closed loop recirculation model to quantify the retention of nanoparticles on the arterial wall after transferring from coated balloons onto the arterial wall under flow conditions. Main components are (a) rat artery (2 cm in length), (b) silicon tubing, and (c) peristaltic pump. (B) Fluorescence imaging of NPs transferred to arteries and (C) spectrophotometric analysis of the studied artery homogenate after NP transfer observed that hydrogel coated balloons transferred a significantly higher amount of nanoparticles to the arterial wall compared to those of dip and LbL coatings. \* $p < 0.05$  vs. LbL, § $p < 0.05$  vs. Hydrogel,  $n = 3$  replicates were used for these studies.

Our NPs might provide a sustained drug release over a month and thereby maintain constant drug bioavailability; however, long term NP retention and drug release when delivered by each coating *in vivo* remains to be investigated.

Several coating methods such as dip coating, spray coating, surface grafting, LbL, and hydrogel coating have been investigated and used to coat the balloon and stent surfaces with drugs, biomolecules, and drug-loaded NPs (Lemos et al., 2013; Brito and Amiji, 2007; Buechel et al., 2012; Hara et al., 2006; Tan et al., 2013). Of those, dip coating is the most commonly employed strategy; however, it often suffers from severe drug loss due to poor interactions between the drug and the coated surface (Acharya and Park, 2006). Our results of NP coatings via LbL coatings also showed significant improvement in NP loading onto the angioplasty balloon and transfer to the arterial wall compared to dip coating (60% and 20% NPs transferred by LbL and dip coatings, respectively). Petersen et al. (2013) have developed and compared three drug coating strategies, namely pipetting, spray coating and dip coating to coat a mixture of paclitaxel and cetylpyridinium salicylate (cetpyrsal) onto angioplasty balloons. These techniques exhibited low drug loss when coated with 50- wt% and 75- wt% of paclitaxel (to cetpyrsal). The correlation between drug loading and drug loss indicated that the pipetting technique, in combination with using 50- wt% paclitaxel concentration for coating, was found to be the ideal combination for coating paclitaxel onto angioplasty balloons. Nakano et al. (2009) used a cationic electrodeposition coating technology to produce a nanoparticle (NP)-eluting drug delivery stent that can overcome the limitations of dip coating. This study also showed that the delivery of PLGA NPs from the NP-eluting stent system had no effect on stent-induced injury, thrombosis, inflammation, or endothelial regeneration *in vivo*, suggesting its potential use in humans without vascular toxicity and/or vascular healing impairment. Additionally, fluorescently labeled PLGA NPs were detectable until four weeks after stent implantation in porcine arteries, indicating an efficient NP retention within the blood vessel.

Another coating technique involves the use of a hydrogel coating on an angioplasty balloon to load and deliver therapeutic reagents.

Hydrogels consist of highly porous structures that permit high drug loading by swelling in aqueous solutions to permit drug loading and by shrinking to release the incorporated drug (Hoare and Kohane, 2008). During the angioplasty procedure, an increase in balloon pressure induces the compressive force on the balloon coated with the hydrogel matrix; thus, resulting in drug expulsion from the hydrogel (Fram et al., 1994). Hydrogel coated drug eluting angioplasty balloons have been widely studied and clinically used for local drug delivery to the arterial wall; thus, reducing the drug dosage and subsequent systemic side-effects. For example, urokinase-coated hydrogel balloons have shown good drug absorption on the balloon, less drug wash-off, great intramural drug delivery, and successful thrombus dissolution in both animal studies and patients with intracoronary thrombus (Mitchel et al., 1994). Similarly, application of heparin-coated hydrogel balloons has shown intramural drug deposition for at least 48 h, leading to the reduction of platelet accumulation and smooth muscle cell proliferation (Azrin et al., 1994). Nunes et al. (1994) compared intravenous (IV) delivery of d-Phe-I-Pro-I-Arginyl chloromethyl ketone (PPACK), an anti-thrombosis drug, with hydrogel coated-angioplasty balloon delivery of PPACK, and observed a higher dose requirement by IV delivery compared to balloon delivery (16 mg of PPACK by IV or 33.5  $\mu$ g of PPACK by hydrogel coating of angioplasty balloons was required to maximize thrombosis inhibition within 45 min). Additionally, IV delivery of anti-thrombosis drugs might produce prolonged bleeding due to high drug doses. Local PPACK delivery using hydrogel coated-balloons could achieve the same therapeutic effect as IV delivery with smaller doses, thereby reducing the potential of bleeding. To further improve drug loading onto the balloon and drug bioavailability, we loaded drugs in nanoparticles and coated drug-loaded NPs onto an angioplasty balloon using acrylic based hydrogel coatings. Acrylic based polymers have been widely used due to their water-soluble, mucoadhesive and bioadhesive properties that allow prolonged retention of the polymer. Additionally, their adhesive nature permits close contact of the tissue with the hydrogel; thus, permitting a local drug release and possibly higher drug penetration into the cells (Calixto and Yoshii, 2015; Kriwet

et al., 1998). The adhesive nature of the hydrogel also ensures adherence of the hydrogel to the balloon surface, while the water-soluble nature of the hydrogel permits diffusion of molecules from the hydrogel to the targeted site (Fram et al., 1994). Furthermore, the abundance of carboxylic groups on the hydrogel surface allows binding of the hydrogel to the cell surface without surface modification with cell adhesion proteins, augmenting drug diffusion from the hydrogel into the extracellular environment (Fram et al., 1994; Chen et al., 2005). Our results highlight the significant improvement in NP delivery and their retention in the arterial lumen using hydrogel coated balloons compared to those of LbL and dip coated balloons under flow conditions; thus, suggesting an improved and efficient technique for vascular drug delivery.

Recent studies have revealed that it is challenging to produce a uniform and thin layer of hydrogel coating on the balloon, and our study also observed the non-uniform hydrogel coating. Kaule et al. (2015) highlighted the influence of the balloon coating structure (namely coating thickness) or the coating material on the performance of angioplasty balloons. This study observed reduced paclitaxel (PTX) loss, and superior PTX transfer in the case of balloons where the PTX was incorporated into a coating matrix of excipients such as cetylpyridinium salicylate (cetpyrsal) (18.94  $\mu\text{m}$  thick) compared to hyaluronic acid (HA) (32.98  $\mu\text{m}$  thick) and Polyvinylpyrrolidone (PVP) (34.11  $\mu\text{m}$ ). They also observed the effects of coating thickness on drug retention, transfer and loss. Cetpyrsal/PTX, which consisted of a thinner and smoother coating, exhibited significantly higher drug transfer compared to the thicker HA/PTX coatings (40% and 22%, respectively). Additionally, the cetpyrsal coatings exhibited lower drug wash-off compared to that of PVP/PTX coatings (28% and 39%, respectively). The drawbacks associated with this research included the difficulty to achieve uniform coatings of NPs onto the balloon surface by both coating techniques, either LbL or hydrogel, and loss of NPs during the coating procedure. Alternate NP coating strategies such as spray coating (Zhu et al., 2010) and ultrasonic spraying (Stryckers et al., 2016) have been found to achieve uniform NP coatings on various surfaces, while being able to control and modulate the coating thickness. These coating techniques could be used in future studies to overcome current limitations. The use of excipients coated onto the angioplasty balloon for carrying drugs has also been studied (Xiong et al., 2016). For example, Lamichhane et al. (2015) investigated the possibility of coating the balloon surface with excipients such as dextran sulfate to effectively load and deliver paclitaxel. Other drug coating strategies, such as the porous matrix coating comprised of iopromide, have also been shown to successfully carry and deploy free paclitaxel during the angioplasty procedure (Granada et al., 2014). These strategies could potentially be applied to coat drug loaded NPs onto angioplasty balloons. Lastly, use of non-biodegradable and synthetic hydrogel materials like acrylic acid limit their biological applications (Gao et al., 2013). To overcome this limitation, use of degradable crosslinkers like phosphazene have been used and observed to render acrylic based gels degradable when subjected to water due to hydrolysis of the crosslinker (Grosse-Sommer and Prud'homme, 1996). Additionally, the cyto-compatible nature of our hydrogel coating could potentially mitigate any biocompatibility issues in case of hydrogel transfer from the balloon surface to the arterial wall. Despite these drawbacks, this work provides critical evidence that NP eluting balloons can be developed as a means to provide local and sustained drug delivery at the arterial wall, while performing vascular interventions such as angioplasty.

## 5. Conclusions

Here we studied three NP formulations and two NP coating strategies to determine the ideal NP-coating combination for DEBs coated with drug-loaded NPs. The combinations were evaluated based on the NP coating efficiency onto the angioplasty balloon and their transfer efficiency from the coatings onto the arterial wall. UPE NPs in

combination with hydrogel coated angioplasty balloons enhanced NP retention and transfer efficiency to the arterial lumen. These NP eluting balloons have demonstrated a significant ability to not only maximize local drug delivery, but also provide sustained *in vitro* drug release. Thus, this strategy could potentially be used in conjunction with an angioplasty procedure to treat atherosclerosis and repair injured blood vessel lumens for cases that DES cannot be applied.

## Acknowledgements

We gratefully acknowledge the support from the National Heart, Lung and Blood Institute grants (U01 HL111146 (KTN), R01 HL118498 (KTN and JY), and T32 HL134613 (KTN; AEK is a fellow of the NIH T32 award)). The content is solely the responsibility of the authors and does not necessarily represent the official views of the National Institutes of Health. We would also like to thank Caleb Shearer and Christian Almdariz (flow system), and Yihui Huang (fluorescence imaging) for their technical assistance.

## References

- Acharya, G., Park, K., 2006. Mechanisms of controlled drug release from drug-eluting stents. *Adv. Drug Deliv. Rev.* 58, 387–401. <https://doi.org/10.1016/j.addr.2006.01.016>.
- Agustina Rodriguez-Granillo, B.R., Rodriguez-Granillo, Gaston, Rodriguez, Alfredo E., 2011. Advantages and disadvantages of biodegradable platforms in drug eluting stents. *World J. Cardiol.* 3, 84–92. <https://doi.org/10.4330/wjc.v3.i3.84>.
- Amin, K., Dannenfels, R.-M., 2006. In vitro hemolysis: Guidance for the pharmaceutical scientist. *J. Pharm. Sci.* 95, 1173–1176. <https://doi.org/10.1002/jps.20627>.
- Azrin, M.A., Mitchel, J.F., Fram, D.B., Pedersen, C.A., Cartun, R.W., Barry, J.J., Bow, L.M., Waters, D.D., McKay, R.G., 1994. Decreased platelet deposition and smooth muscle cell proliferation after intramural heparin delivery with hydrogel-coated balloons. *Circulation* 90, 433–441. <https://doi.org/10.1161/01.CIR.90.1.433>.
- Brito, L., Amiji, M., 2007. Nanoparticulate carriers for the treatment of coronary restenosis. *Int. J. Nanomed.* 2, 143–161.
- Buechel, R., Stirnimann, A., Zimmer, R., Keo, H., Groechenig, E., 2012. Drug-eluting stents and drug-coated balloons in peripheral artery disease. *Vasa* 41, 248–261. <https://doi.org/10.1024/0301-0526/a000200>.
- Byrne, R.A., Neumann, F.-J., Mehilli, J., Piniček, S., Wolff, B., Tiroch, K., Schulz, S., Fusaro, M., Ott, I., Ibrahim, T., 2013. Paclitaxel-eluting balloons, paclitaxel-eluting stents, and balloon angioplasty in patients with restenosis after implantation of a drug-eluting stent (ISAR-DESIRE 3): a randomised, open-label trial. *Lancet* 381, 461–467. [https://doi.org/10.1016/S0140-6736\(12\)61964-3](https://doi.org/10.1016/S0140-6736(12)61964-3).
- Calixto, G., Yoshii, A.C., Rocha e Silva, H., Stringhetti Ferreira Cury, B., Chorilli, M., 2015. Polyacrylic, acid polymers hydrogels intended to topical drug delivery: Preparation and characterization. *Pharm. Dev. Technol.* 20, 490–496. <https://doi.org/10.3109/10837450.2014.882941>.
- Chen, Y.M., Shiraishi, N., Satokawa, H., Kakugo, A., Narita, T., Gong, J.P., Osada, Y., Yamamoto, K., Ando, J., 2005. Cultivation of endothelial cells on adhesive protein-free synthetic polymer gels. *Biomaterials* 26, 4588–4596. <https://doi.org/10.1016/j.biomaterials.2004.11.025>.
- Cyrus, T., Zhang, H., Allen, J.S., Williams, T.A., Hu, G., Caruthers, S.D., Wickline, S.A., Lanza, G.M., 2008. Intramural delivery of rapamycin with  $\alpha\text{v}\beta3$ -targeted paramagnetic nanoparticles inhibits stenosis after balloon injury. *Arterioscler. Thromb. Vasc. Biol.* 28, 820–826. <https://doi.org/10.1161/ATVBAHA.107.156281>.
- Davda, J., Labhasetwar, V., 2002. Characterization of nanoparticle uptake by endothelial cells. *Int. J. Pharm.* 233, 51–59. [https://doi.org/10.1016/S0378-5173\(01\)00923-1](https://doi.org/10.1016/S0378-5173(01)00923-1).
- Dey, J., Xu, H., Shen, J., Thevenot, P., Gondi, S.R., Nguyen, K.T., Sumerlin, B.S., Tang, L., Yang, J., 2008. Development of biodegradable crosslinked urethane-doped polyester elastomers. *Biomaterials* 29, 4637–4649. <https://doi.org/10.1016/j.biomaterials.2008.08.020>.
- Dey, J., Xu, H., Nguyen, K.T., Yang, J., 2010. Crosslinked urethane doped polyester bi-phasic scaffolds: potential for in vivo vascular tissue engineering. *J. Biomed. Mater. Res. A* 95A, 361–370. <https://doi.org/10.1002/jbm.a.32846>.
- Fanggiday, J.C., Stella, P.R., Guyomi, S.H., Doevendans, P.A., 2008. Safety and efficacy of drug-eluting balloons in percutaneous treatment of bifurcation lesions the DEBIUT (drug-eluting balloon in bifurcation utrecht) registry. *Catheter Cardiovasc. Interv.* 71, 629–635. <https://doi.org/10.1002/ccd.21452>.
- Finke, J.H., Richter, C., Gothsch, T., Kwade, A., Büttgenbach, S., Müller-Goymann, C.C., 2014. Coumarin 6 as a fluorescent model drug: how to identify properties of lipid colloidal drug delivery systems via fluorescence spectroscopy? *Eur. J. Lipid Sci. Technol.* 116, 1234–1246. <https://doi.org/10.1002/ejlt.201300413>.
- Fram, D.B., Aretz, T., Azrin, M.A., Mitchel, J.F., Samady, H., Gillam, L.D., Sahatjian, R., Waters, D., McKay, R.G., 1994. Localized intramural drug delivery during balloon angioplasty using hydrogel-coated balloons and pressure-augmented diffusion. *J. Am. Coll. Cardiol.* 23, 1570–1577. [https://doi.org/10.1016/0735-1097\(94\)90658-0](https://doi.org/10.1016/0735-1097(94)90658-0).
- Gao, X., He, C., Xiao, C., Zhuang, X., Chen, X., 2013. Biodegradable pH-responsive polyacrylic acid derivative hydrogels with tunable swelling behavior for oral delivery of insulin. *Polymer* 54, 1786–1793. <https://doi.org/10.1016/j.polymer.2013.01.050>.

- Granada, J.F., Stenoien, M., Buszman, P.P., Tellez, A., Langanki, D., Kaluza, G.L., Leon, M.B., Gray, W., Jaff, M.R., Schwartz, R.S., 2014. Mechanisms of tissue uptake and retention of paclitaxel-coated balloons: Impact on neointimal proliferation and healing. *e000117*. <https://doi.org/10.1136/openhrt-2014-000117>.
- Grosse-Sommer, A., Prud'homme, R.K., 1996. Degradable phosphazene-crosslinked hydrogels. *J. Control. Rel.* 40, 261–267. [https://doi.org/10.1016/0168-3659\(95\)00193-X](https://doi.org/10.1016/0168-3659(95)00193-X).
- Guzman, L.A., Labhasetwar, V., Song, C., Jang, Y., Lincoff, A.M., Levy, R., Topol, E.J., 1996. Local intraluminal infusion of biodegradable polymeric nanoparticles. A novel approach for prolonged drug delivery after balloon angioplasty. *Circulation* 94, 1441–1448. <https://doi.org/10.1161/01.cir.94.6.1441>.
- Guzman, L.A., Labhasetwar, V., Song, C., Jang, Y., Lincoff, A.M., Levy, R., Topol, E.J., 1996. Local intraluminal infusion of biodegradable polymeric nanoparticles: a novel approach for prolonged drug delivery after balloon angioplasty. *Circulation* 94, 1441–1448. <https://doi.org/10.1161/01.CIR.94.6.1441>.
- Hara, H., Nakamura, M., Palmaz, J.C., Schwartz, R.S., 2006. Role of stent design and coatings on restenosis and thrombosis. *Adv. Drug Deliv. Rev.* 58, 377–386. <https://doi.org/10.1016/j.addr.2006.01.022>.
- Herdeg, C.G.T., Goehring-Frischholz, K., Zuern, C., Hartmann, U., Haase, K.K., Gawaz, M., 2008. Catheter-based local antiproliferative therapy in kissing balloon technique for in-stent stenosis of coronary artery bifurcation lesions. *Can. J. Cardiol.* 24, 309–311. [https://doi.org/10.1016/S0828-282X\(08\)70182-X](https://doi.org/10.1016/S0828-282X(08)70182-X).
- Hoare, T.R., Kohane, D.S., 2008. Hydrogels in drug delivery: progress and challenges. *Polymer* 49, 1993–2007. <https://doi.org/10.1016/j.polymer.2008.01.027>.
- Hu, J., Guo, J., Xie, Z., Shan, D., Gerhard, E., Qian, G., Yang, J., 2016. Fluorescence imaging enabled poly(lactide-co-glycolide). *Acta Biomater.* 29, 307–319. <https://doi.org/10.1016/j.actbio.2015.10.010>.
- Humphrey, W.R., Erickson, L.A., Simmons, C.A., Northrup, J.L., Wishka, D.G., Morris, J., Labhasetwar, V., Song, C., Levy, R.J., Shebuski, R.J., 1997. The effect of intraluminal delivery of polymeric nanoparticles loaded with the antiproliferative 2-aminochromone U-86983 on neointimal hyperplasia development in balloon-injured porcine coronary arteries. *Adv. Drug Deliv. Rev.* 24, 87–108. [https://doi.org/10.1016/S0169-409X\(96\)00484-X](https://doi.org/10.1016/S0169-409X(96)00484-X).
- Imanishi, T., Arita, M., Tomobuchi, Y., Hamada, M., Hano, T., Nishio, I., 1997. Effects of locally administered argatroban on restenosis after balloon angioplasty: experimental and clinical study. *Clin. Exp. Pharmacol. Physiol.* 24, 800–806. <https://doi.org/10.1111/j.1440-1681.1997.tb02694.x>.
- Jabbari, E., Tavakoli, J., Sarvestani, A.S., 2007. Swelling characteristics of acrylic acid polyelectrolyte hydrogel in a dc electric field. *Smart Mater. Struct.* 16, 1614. <https://doi.org/10.1088/0964-1726/16/5/015>.
- Kaule, S., Minrath, I., Stein, F., Kragl, U., Schmidt, W., Schmitz, K.-P., Sternberg, K., Petersen, S., 2015. Correlating coating characteristics with the performance of drug-coated balloons—A comparative in vitro investigation of own established hydrogel- and ionic liquid-based coating matrices. *e0116080*. <https://doi.org/10.1371/journal.pone.0116080>.
- Kona, S., Specht, D., Rahimi, M., Shah, B.P., Gilbertson, T.A., Nguyen, K.T., 2012. Targeted biodegradable nanoparticles for drug delivery to smooth muscle cells. *J. Nanosci. Nanotechnol.* 12, 236–244. <https://doi.org/10.1166/jnn.2012.5131>.
- Kona, S., Dong, J.-F., Liu, Y., Tan, J., Nguyen, K.T., 2012. Biodegradable nanoparticles mimicking platelet binding as a targeted and controlled drug delivery system. *Int. J. Pharm.* 423, 516–524. <https://doi.org/10.1016/j.ijpharm.2011.11.043>.
- Kriwet, B., Walter, E., Kissel, T., 1998. Synthesis of bioadhesive poly(acrylic acid) nano- and microparticles using an inverse emulsion polymerization method for the entrapment of hydrophilic drug candidates. *J. Control. Rel.* 56, 149–158. [https://doi.org/10.1016/S0168-3659\(98\)00078-9](https://doi.org/10.1016/S0168-3659(98)00078-9).
- Labhasetwar, V., Song, C., Levy, R.J., 1997. Nanoparticle drug delivery system for restenosis. *Adv. Drug Deliv. Rev.* 24, 63–85. [https://doi.org/10.1016/S0169-409X\(96\)00483-8](https://doi.org/10.1016/S0169-409X(96)00483-8).
- Labhasetwar, V., Song, C., Humphrey, W., Shebuski, R., Levy, R.J., 1998. Arterial uptake of biodegradable nanoparticles: effect of surface modifications. *J. Pharm. Sci.* 87, 1229–1234. <https://doi.org/10.1021/js980021f>.
- Lamichhane, S., Anderson, J., Remund, T., Kelly, P., Mani, G., 2015. Dextran sulfate as a drug delivery platform for drug-coated balloons: Preparation, characterization, in vitro drug elution, and smooth muscle cell response. *J. Biomed. Mater. Res. B Appl. Biomater.* 104, 1416–1430. <https://doi.org/10.1002/jbm.b.33494>.
- Latib, A., Colombo, A., Castriota, F., Micari, A., Cremonesi, A., De Felice, F., Marchese, A., Tespili, M., Presbitero, P., Sgueglia, G.A., Buffoli, F., Tamburino, C., Varbella, F., Menozzi, A., 2012. A randomized multicenter study comparing a paclitaxel drug-eluting balloon with a paclitaxel-eluting stent in small coronary vessels: the BELLO (Balloon Elution and Late Loss Optimization) study. *J. Am. Coll. Cardiol.* 60, 2473–2480. <https://doi.org/10.1016/j.jacc.2012.09.020>.
- Lemos, P.A., Farooq, V., Takimura, C.K., Gutierrez, P.S., Virmani, R., Kolodgie, F., Christians, U., Kharlamov, A., Doshi, M., Sojitra, P., 2013. Emerging technologies: Polymer-free phospholipid encapsulated sirolimus nanocarriers for the controlled release of drug from a stent-plus-balloon or a stand-alone balloon catheter. *EuroIntervention* 9, 146–156. <https://doi.org/10.4244/EIJV9I1A21>.
- Lin, A., Sabis, A., Kona, S., Nattama, S., Patel, H., Dong, J.F., Nguyen, K.T., 2010. Shear-regulated uptake of nanoparticles by endothelial cells and development of endothelial-targeting nanoparticles. *J. Biomed. Mater. Res. A* 93, 833–842. <https://doi.org/10.1002/jbm.a.32592>.
- Menon, J.U., Ravikumara, P., Pise, A., Gyawali, D., Hsia, C.C.W., Nguyen, K.T., 2014. Polymeric nanoparticles for pulmonary protein and DNA delivery. *Acta Biomater.* 10, 2643–2652. <https://doi.org/10.1016/j.actbio.2014.01.033>.
- Mitchell, J.F., Azrin, M.A., Fram, D.B., Hong, M.K., Wong, S.C., Barry, J.J., Bow, L.M., Curley, T.M., Kiernan, F.J., Waters, D.D., 1994. Inhibition of platelet deposition and lysis of intracoronary thrombus during balloon angioplasty using urokinase-coated hydrogel balloons. *Circulation* 90, 1979–1988. <https://doi.org/10.1161/01.CIR.90.4.1979>.
- Mu, L., Feng, S.S., 2003. A novel controlled release formulation for the anticancer drug paclitaxel (Taxol®): PLGA nanoparticles containing vitamin E TPGS. *J. Control. Rel.* 86, 33–48. [https://doi.org/10.1016/S0168-3659\(02\)00320-6](https://doi.org/10.1016/S0168-3659(02)00320-6).
- Nakano, K., Egashira, K., Masuda, S., Funakoshi, K., Zhao, G., Kimura, S., Matoba, T., Sueishi, K., Endo, Y., Kawashima, Y., 2009. Formulation of nanoparticle-eluting stents by a cationic electrodeposition coating technology: Efficient nano-drug delivery via bioabsorbable polymeric nanoparticle-eluting stents in porcine coronary arteries. *JACC Cardiovasc. Interv.* 2, 277–283. <https://doi.org/10.1016/j.jcin.2008.08.023>.
- Nguyen, K.T., Su, S.H., Sheng, A., Wawro, D., Schwade, N.D., Brouse, C.F., Greilich, P.E., Tang, L., Eberhart, R.C., 2003. In vitro hemocompatibility studies of drug-loaded poly(L-lactide acid) fibers. *Biomaterials* 24, 5191–5201.
- Nunes, G.L., Hanson, S.R., King III, S.B., Sahatjian, R.A., Scott, N.A., 1994. Local delivery of a synthetic antithrombin with a hydrogel-coated angioplasty balloon catheter inhibits platelet-dependent thrombosis. *J. Am. Coll. Cardiol.* 23, 1578–1583. [https://doi.org/10.1016/0735-1097\(94\)90659-9](https://doi.org/10.1016/0735-1097(94)90659-9).
- Panyam, J., Dali, M.M., Sahoo, S.K., Ma, W., Chakravarthi, S.S., Amidon, G.L., Levy, R.J., Labhasetwar, V., 2003. Polymer degradation and in vitro release of a model protein from poly(D, L-lactide-co-glycolide) nano- and microparticles. *J. Control. Rel.* 92, 173–187. [https://doi.org/10.1016/S0168-3659\(03\)00328-6](https://doi.org/10.1016/S0168-3659(03)00328-6).
- Panyam, J., Labhasetwar, V., 2003. Biodegradable nanoparticles for drug and gene delivery to cells and tissue. *Adv. Drug Deliv. Rev.* 55, 329–347. [https://doi.org/10.1016/S0169-409X\(02\)00228-4](https://doi.org/10.1016/S0169-409X(02)00228-4).
- Papaioannou, T.G., Stefanadis, C., 2005. Vascular wall shear stress: Basic principles and methods. *Hellenic J. Cardiol.* 46, 9–15.
- Petersen, S., Kaule, S., Stein, F., Minrath, I., Schmitz, K.-P., Kragl, U., Sternberg, K., 2013. Novel paclitaxel-coated angioplasty balloon catheter based on cetylpyridinium salicylate: preparation, characterization and simulated use in an in vitro vessel model. *Mater. Sci. Eng. C Mater. Biol. Appl.* 33, 4244–4250. <https://doi.org/10.1016/j.msec.2013.06.021>.
- Rittger, H., Brachmann, J., Sinha, A.-M., Waliszewski, M., Ohlow, M., Brugger, A., Thiele, H., Birkemeyer, R., Kurowski, V., Breithardt, O.-A., 2012. A randomized, multicenter, single-blinded trial comparing paclitaxel-coated balloon angioplasty with plain balloon angioplasty in drug-eluting stent restenosis: the PEPCAD-DES study. *J. Am. Coll. Cardiol.* 59, 1377–1382. <https://doi.org/10.1016/j.jacc.2012.01.015>.
- Roger, V.L., Go, A.S., Lloyd-Jones, D.M., Benjamin, E.J., Berry, J.D., Borden, W.B., Bravata, D.M., Dai, S., Ford, E.S., Fox, C.S., 2012. Heart disease and stroke statistics—2012 update: a report from the American Heart Association. *Circulation* 125, e2–e220. <https://doi.org/10.1161/CIR.0b013e31823ac046>.
- Rolland, P.H., Mekkaoui, C., Palassi, M., Friggi, A., Moulin, G., Piquet, P., Bartoli, J.-M., 2003. Efficacy of local molsidomine delivery from a hydrogel-coated angioplasty balloon catheter in the atherosclerotic porcine model. *Cardiovasc. Intervent. Radiol.* 26, 65–72. <https://doi.org/10.1007/s00270-002-1940-y>.
- Scheller, B., Hehrlein, C., Bocksch, W., Rutsch, W., Haghi, D., Dietz, U., Böhm, M., Speck, U., 2006. Treatment of coronary in-stent restenosis with a paclitaxel-coated balloon catheter. *N. Engl. J. Med.* 355, 2113–2124. <https://doi.org/10.1056/NEJMoa061254>.
- Song, C., Labhasetwar, V., Cui, X., Underwood, T., Levy, R.J., 1998. Arterial uptake of biodegradable nanoparticles for intravascular local drug delivery: results with an acute dog model. *J. Control. Rel.* 54, 201–211. [https://doi.org/10.1016/S0168-3659\(98\)00016-9](https://doi.org/10.1016/S0168-3659(98)00016-9).
- Stryckers, J., D'Olielsaeger, L., Silvano, J., Apolinario, C., Laranjeiro, A., Gruber, J., D'Haen, J., Manca, J., Ethirajan, A., Deferme, W., 2016. Layer formation and morphology of ultrasonic spray coated polystyrene nanoparticle layers. *Phys. status solidi a* 213, 1441–1446. <https://doi.org/10.1002/pssa.201533026>.
- Su, L.-C., Xu, H., Tran, R.T., Tsai, Y.-T., Tang, L., Banerjee, S., Yang, J., Nguyen, K.T., 2014. In situ re-endothelialization via multifunctional nanoscaffolds. *ACS Nano* 8, 10826–10836. <https://doi.org/10.1021/nn504636n>.
- Tan, A., Farhatnia, Y., de Mel, A., Rajadas, J., Alavijeh, M.S., Seifalian, A.M., 2013. Inception to actualization: next generation coronary stent coatings incorporating nanotechnology. *J. Biotechnol.* 164, 151–170. <https://doi.org/10.1016/j.jbiotec.2013.01.020>.
- Vasir, J.K., Labhasetwar, V., 2006. Polymeric nanoparticles for gene delivery. *Exp. Opin. Drug Deliv.* 3, 325–344. <https://doi.org/10.1517/17425247.3.3.325>.
- Vasir, J.K., Labhasetwar, V., 2007. Biodegradable nanoparticles for cytosolic delivery of therapeutics. *Adv. Drug Deliv. Rev.* 59, 718–728. <https://doi.org/10.1016/j.addr.2007.06.003>.
- Wadajkar, A.S., Kadapure, T., Zhang, Y., Cui, W., Nguyen, K.T., Yang, J., 2012. Dual-imaging enabled cancer-targeting nanoparticles. *Adv. Healthc. Mater.* 1, 450–456. <https://doi.org/10.1002/adhm.201100055>.
- Waksman, R., Pakala, R., 2009. Drug-eluting balloon: the comeback kid? *Circ. Cardiovasc. Interv.* 2, 352–358. <https://doi.org/10.1161/CIRCINTERVENTIONS.109.873703>.
- Waxman, K., Mason, G.R., Tremper, K.K., 1985. Blood and plasma substitutes—Plasma expansion and oxygen transport properties. *West. J. Med.* 143, 202–206.
- Westedt, U., Barbu-Tudoran, L., Schaper, A.K., Kalinowski, M., Alfke, H., Kissel, T., 2002. Deposition of nanoparticles in the arterial vessel by porous balloon catheters: localization by confocal laser scanning microscopy and transmission electron microscopy. *AAPS PharmSci.* 4, 206–211. <https://doi.org/10.1208/ps040441>.
- Wilensky, R.L., March, K.L., Gradus-Pizlo, I., Schauwecker, D., Michaels, M., Robinson, J., Carlson, K., Hathaway, D.R., 1995. Regional and arterial localization of radioactive microparticles after local delivery by unsupported or supported porous balloon catheters. *Am. Heart J.* 129, 852–859. [https://doi.org/10.1016/0002-8703\(95\)90103-5](https://doi.org/10.1016/0002-8703(95)90103-5).

Xiong, G.M., Ang, H., Lin, J., Lui, Y.S., Phua, J.L., Chan, J.N., Venkatraman, S., Foin, N., Huang, Y., 2016. Materials technology in drug eluting balloons: current and future perspectives. *J. Control. Rel.* 239, 92–106. <https://doi.org/10.1016/j.jconrel.2016.08.018>.

Xu, H., Kona, S., Su, L.-C., Tsai, Y.-T., Dong, J.-F., Brilakis, E.S., Tang, L., Banerjee, S., Nguyen, K.T., 2013. Multi-ligand poly (L-lactic-co-glycolic acid) nanoparticles inhibit

activation of endothelial cells. *J. Cardiovasc. Transl. Res.* 6, 570–578. <https://doi.org/10.1007/s12265-013-9460-5>.

Zhu, D., Jin, X., Leng, X., Wang, H., Bao, J., Liu, W., Yao, K., Song, C., 2010. Local gene delivery via endovascular stents coated with dodecylated chitosan-plasmid DNA nanoparticles. *Int. J. Nanomed.* 5, 1095–1102. <https://doi.org/10.2147/IJN.S14358>.